



# Stable Isotope Resolved Metabolomics Reveals the Role of Anabolic and Catabolic Processes in Glyphosate-Induced Amino Acid Accumulation in *Amaranthus palmeri* Biotypes

Amith Maroli,<sup>†</sup> Vijay Nandula,<sup>§</sup> Stephen Duke,<sup>Δ</sup> and Nishanth Tharayil<sup>\*,†</sup>

<sup>†</sup>Department of Plant & Environmental Sciences, Clemson University, Clemson, South Carolina 29634, United States

<sup>§</sup>Crop Production Systems Research Unit, U.S. Department of Agriculture, Stoneville, Mississippi 38776, United States

<sup>Δ</sup>Natural Products Utilization Research Unit, Agricultural Research Service, U.S. Department of Agriculture, Oxford, Mississippi 38677, United States

## Supporting Information

**ABSTRACT:** Biotic and abiotic stressors often result in the buildup of amino acid pools in plants, which serve as potential stress mitigators. However, the role of anabolic (de novo amino acid synthesis) versus catabolic (proteolytic) processes in contributing to free amino acid pools is less understood. Using stable isotope-resolved metabolomics (SIRM), we measured the de novo amino acid synthesis in glyphosate susceptible (S-) and resistant (R-) *Amaranthus palmeri* biotypes. In the S-biotype, glyphosate treatment at 0.4 kg ae/ha resulted in an increase in total amino acids, a proportional increase in both <sup>14</sup>N and <sup>15</sup>N amino acids, and a decrease in soluble proteins. This indicates a potential increase in de novo amino acid synthesis, coupled with a lower protein synthesis and a higher protein catabolism following glyphosate treatment in the S-biotype. Furthermore, the ratio of glutamine/glutamic acid (Gln/Glu) in the glyphosate-treated S- and R-biotypes indicated that the initial assimilation of inorganic nitrogen to organic forms is less affected by glyphosate. However, amino acid biosynthesis downstream of glutamine is disproportionately disrupted in the glyphosate treated S-biotype. It is thus concluded that the herbicide-induced amino acid abundance in the S-biotype is contributed by both protein catabolism and de novo synthesis of amino acids such as glutamine and asparagine.

**KEYWORDS:** <sup>15</sup>N isotopologue, LC-MS/MS, *Amaranthus palmeri*, amino acid accumulation, anabolic and catabolic processes, de novo biosynthesis

## INTRODUCTION

Amino acids are the building blocks of proteins, and they also serve as precursors of nitrogen-containing metabolites, including nucleic acids, polyamines, quaternary ammonium compounds, and some hormones. In addition to their primary role in growth and nitrogen transportation, amino acids play a critical role as regulatory and signaling compounds and facilitate homeostasis when plants are subjected to biotic and abiotic stresses.<sup>1</sup> In plants, under environmental stress, de novo protein synthesis is generally inhibited, and protein turnover and proteolytic activity are increased, resulting in an increased level of total free amino acids.<sup>2–4</sup> Also, environmental stress, by affecting plant metabolic pathways, can influence the de novo synthesis of amino acids. The higher cellular concentration of free amino acids is thought to contribute to the overall stress mitigation strategy in plants through their role as osmoregulators, ion uptake modulators, and hormone biosynthesis regulators.<sup>5–7</sup> Although the catabolic versus anabolic pathways that contribute to the greater physiological concentration of amino acids could differentially influence the overall performance of plants under stressful environments, we currently lack a robust understanding of the relative contribution of these pathways to the buildup of amino acid pools.

Present-day agriculture relies heavily on herbicides for management of weeds. Of the several classes of herbicides that target various vital plant metabolic processes, N-

(phosphonomethyl)glycine (glyphosate), the compound that competitively inhibits the enzyme 5-enolpyruvylshikimate-3-phosphate synthase (EPSPS) and thus disrupts aromatic amino acid synthesis, is the most widely used herbicide worldwide.<sup>8</sup> Inhibition of EPSPS results in blockage of the shikimate pathway, resulting in accumulation of shikimic acid and depletion of aromatic amino acid pools.<sup>9</sup> Furthermore, inhibition of the shikimate pathway not only reduces aromatic amino acid biosynthesis but also disrupts other physiological processes such as photosystem II quantum efficiency and photosynthetic carbon fixation, thereby interfering with the movement of assimilated carbon.<sup>10,11</sup> Although several studies have confirmed the nontargeted effects of glyphosate in plants, the secondary effects of EPSPS inhibition are poorly understood.<sup>2,12,13</sup> Because the carbon backbones of amino acids are derived from carbon metabolic pathways, the inhibition of EPSPS also has the potential to interfere with the synthesis of nonaromatic amino acids.<sup>14</sup> A few studies have demonstrated that an exogenous supply of amino acids (branched chain and aromatic) following the application of amino acid synthesis-inhibiting herbicides can not only prevent the inhibition of

Received: May 15, 2016

Revised: July 26, 2016

Accepted: July 29, 2016

Published: July 29, 2016

growth in plants, but also could reverse herbicidal toxicity.<sup>15,16</sup> However, total amino acid pools in weed and crop biotypes that are tolerant, susceptible, or resistant to glyphosate generally increase following glyphosate application.<sup>14,17,18</sup> Considering the contrasting degrees of EPSPS inhibition by glyphosate in susceptible (S-) and resistant (R-) biotypes, the observed initial increase in free amino acid concentration in both of these biotypes following glyphosate application challenges our understanding of the early effects of EPSPS inhibitors on cellular metabolism. Following the application of glyphosate, anabolic vs catabolic metabolism could contribute differentially to the overall amino acid pools in R- and S-biotypes, which is currently less known.

To characterize the differential contribution of anabolic (de novo synthesis) versus catabolic (proteolysis) processes to the total amino acid pools, the current study examined the fluxes in amino acid pools in *Amaranthus palmeri* biotypes susceptible and resistant to glyphosate. We hypothesized that the elevated amino acid pool observed in the R-biotype following glyphosate application would be primarily due to increased de novo synthesis, whereas the observed increase in the amino acid pool of the S-biotype would mainly be contributed by protein catabolism.

## MATERIALS AND METHODS

**Plant Biotypes and Experimental Design.** Seeds of *A. palmeri* that are susceptible (S-) or resistant (R-) to the recommended field application rate of glyphosate (0.84 kg ae/ha) were obtained from the Crop Production Systems Research Unit (USDA-ARS, Stoneville, MS, USA). The GR<sub>50</sub> values of S- and R-biotypes were 0.09 and 1.3 kg ae/ha of glyphosate, respectively (~15-fold resistance in the R-biotype).<sup>19</sup> Seeds were germinated in a commercial germination mixture in a greenhouse maintained at 30/20 °C day/night temperatures with a 14 h photoperiod. A week after germination, individual seedlings were transplanted to 250 mL glass Erlenmeyer flasks containing 0.5× Murashige and Skoog (MS) modified basal salt mixture without nitrogen (PhytoTechnology Laboratories, Shawnee Mission, KS, USA), and was supplemented with 3 mM <sup>14</sup>N ammonium nitrate solution. The hydroponic systems were constantly aerated with the solution changed at 5-day intervals and were maintained under similar greenhouse conditions as above. A week after transplanting, both biotypes were randomly assigned to two treatment groups, glyphosate treated and water treated. Glyphosate (Roundup ProMax) (Monsanto Co., St. Louis, MO, USA) was sprayed at a rate of 0.4 kg ae/ha, which corresponds to approximately half the recommended field application rate of glyphosate. The control plants were treated with water.

Before application of either water or herbicide, the roots of plants were carefully rinsed multiple times with deionized water, and the plants were held in nitrogen-free Hoagland's solution for 8 h in darkness to reduce the endogenous <sup>14</sup>N mineral nitrogen pool. Respective treatments (water or glyphosate) were applied to 12 plants/biotype using an enclosed spray chamber (DeVries Manufacturing, Hollandale, MN, USA) calibrated to deliver 374 L/ha through an 8001E flat fan nozzle (Tee Jet Spraying Systems Co., Wheaton, IL, USA). At the time of treatment application, both S- and R-biotypes were morphologically similar and were ~20 cm tall with similar numbers of leaves. Following treatment application, six plants from each treatment per biotype were transferred to a modified MS solution supplemented with 3 mM <sup>14</sup>N-ammonium nitrate, whereas the remaining six plants were transferred to modified MS solution supplemented with 3 mM <sup>15</sup>NH<sub>4</sub><sup>15</sup>NO<sub>3</sub> (>98 atom % <sup>15</sup>N<sub>2</sub>) (Cambridge Isotope Laboratories, Tewksbury, MA, USA). All plants were held under greenhouse conditions as specified above. Three young apical leaves along with the meristem were harvested individually from all six plants per glyphosate and control treatments at 36 h after treatment (HAT, after exposure to 28 h sunlight over two

days), stored at -80 °C, and ground to a fine powder with dry ice before analyses.

**Analysis of Amino Acids and Proteins.** Total soluble protein (TSP) and amino acids in the ground leaf tissues were extracted as described by Maroli et al.<sup>20</sup> and the TSP content was estimated by bicinchoninic acid (BCA) assay according to the manufacturer's recommended protocol (BCA Protein Assay kit; Pierce Chemical Co., Rockford, IL, USA). Amino acid isotopes were chromatographically separated and analyzed using a Shimadzu Ultra-Fast liquid chromatograph, equipped with a degasser and autosampler connected in tandem to a triple-quadrupole mass spectrometer through an electrospray ionization interface (UFLC-ESI-MS/MS; Shimadzu 8030). The chromatographic separations of amino acids were achieved on a 100 mm × 3 mm i.d. × 2.6 μm, Kinetex XB-C18 column (Phenomenex, Torrance, CA, USA) using 0.05% formic acid (solvent A) and methanol (solvent B). The solvent flow rate was maintained at 0.3 mL/min with a gradient program where solvent B was initially held at 4% for 2 min, increased at a rate of 2% solvent B per minute for the next 7 min, followed by an increase in solvent B at a rate of 6% per minute for the next 5 min, and re-equilibrated at 4% B for 7 min. Tandem mass spectrometry experiments were performed on a triple-quadrupole tandem mass spectrometer. Single-ion transitions (*m/z*) for each of the <sup>14</sup>N and <sup>15</sup>N amino acids were optimized using authentic <sup>14</sup>N- and <sup>15</sup>N-labeled amino acid standards (cell free amino acid mixture-<sup>15</sup>N (98 atom % <sup>15</sup>N)) (Aldrich Chemicals, Sigma-Aldrich Co., St. Louis, MO, USA). Fragmentation of parent ion peaks was carried out at different collision energies ranging from -15 to -40 V at 5 V intervals to select the ideal transitions that provided the highest signal intensity with a dominant fragment ion. The optimized multiple reaction monitoring (MRM) was used to analyze the amino acid composition of the samples. The mass spectrometer parameters were as follows: desolvation line (DL) temperature maintained at 250 °C, heat block at 400 °C, capillary voltage at 22 kV, nebulizing gas of nitrogen at 3 L/min, and curtain gas nitrogen at a rate of 10 L/min.

**Analysis of Polar Metabolites.** Metabolite profiling of the leaves was carried out on a GC-MS as described previously.<sup>20</sup> Briefly, 100 mg of finely powdered leaf tissues was extracted with 1 mL of methanol by sonication in an ice bath. The supernatant was transferred into glass tubes, and the polar metabolites were separated by adding an equal volume of chloroform, followed by water. Subsamples (150 μL) of the top aqueous-methanol phase were transferred into glass inserts, and 5 μL of 5 mg/mL ribitol (internal standard) in hexane and 5 μL of 5 mg/mL of D<sub>27</sub>-myristic acid (retention time lock) in hexane were added and then completely dried under nitrogen. Dried samples were methoxylaminated at 60 °C with 20 μL of methoxylamine hydrochloride (20 mg/mL) in pyridine for 90 min and further silylated with 90 μL of *N*-methyl-*N*-(trimethylsilyl)trifluoroacetamide (MSTFA) with 1% trimethylchlorosilane (TMCS) for 30 min at 40 °C. The metabolites were separated on a 30 m × 0.25 mm i.d. × 0.25 μm, J&W DB-5 ms, column (Agilent Technologies, Santa Clara, CA, USA) and analyzed using a model 7980 gas chromatograph (Agilent Technologies) coupled to a 5975 C series quadrupole mass detector (Agilent Technologies). The initial oven temperature was maintained at 60 °C for 1 min, followed by temperature ramp at 10 °C/min to 300 °C, with a 7 min hold at 300 °C. Metabolite peaks were identified by comparing the absolute retention time, retention time index of the sample with that of the in-house metabolites library supplemented with Fiehn Library (Agilent Technologies, Wilmington, DE, USA).

**<sup>15</sup>N-Amino Acid Isotopologue Enrichment Calculation.** Peak areas for the monoisotopic peak (*m*) and first isotope (*m* + 1) of all observed amino acids, as well as the second isotope (*m* + 2) for Gln and Asn, were determined using Shimadzu LabSolutions v2.04 software (Shimadzu, Kyoto, Japan). Theoretical values of the isotopic ratios <sup>13</sup>C isotope contribution (%) for each amino acid were calculated using the MS-Isotope tool in Protein Prospector, and these values were used to correct the *m* + 1 peak area for all amino acids except Gln and Asn, for which the *m* + 1 correction was applied to the *m* + 2 peak area for both the *m* peak and the isotopically labeled portion of the *m* + 1 peak as given in Table T1 of the [Supporting Information](#).<sup>21,22</sup> The *m* peak area corresponds to the <sup>14</sup>N amino acid

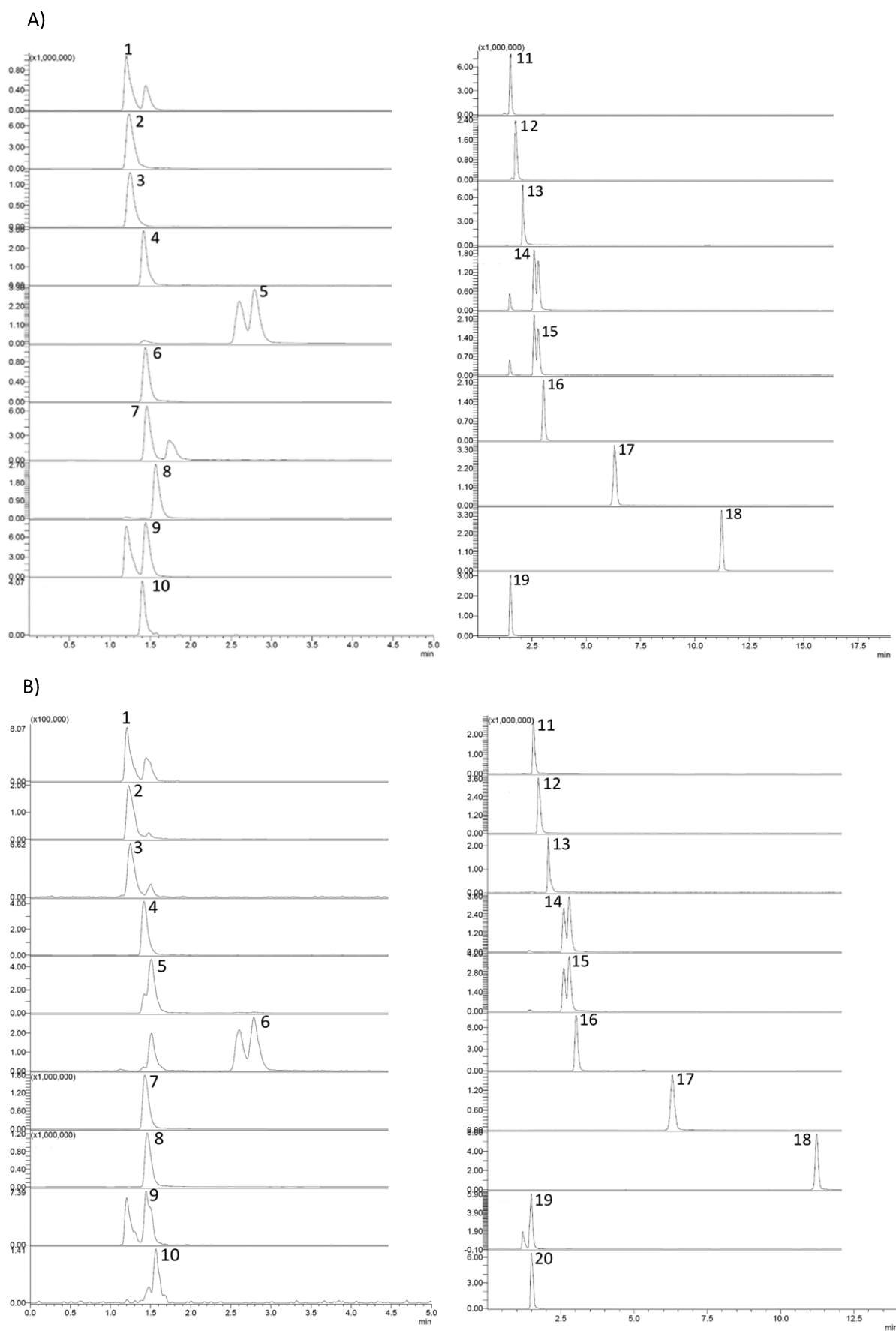


**Figure 1.** LC-MS chromatogram for the identification of  $^{14}\text{N}$  and  $^{15}\text{N}$  amino acids. (A) Mass spectra of  $^{14}\text{N}$  amino acids. Numbers correspond to the amino acids (1) lysine, (2) histidine, (3) arginine, (4) serine, (5) asparagine, (6) alanine, (7) threonine, (8) proline, (9) glutamine, (10) glycine,

Figure 1. continued

(11) glutamic acid, (12) valine, (13) methionine, (14) isoleucine, (15) leucine, (16) tyrosine, (17) phenylalanine, (18) tryptophan, and (19) aspartic acid. (B) Mass spectra of  $^{15}\text{N}$ -amino acids. Numbers correspond to the amino acids (1) lysine, (2) histidine, (3) arginine, (4) serine, (5)  $\text{N}_2$ -asparagine, (6) asparagine, (7) alanine, (8) threonine, (9) glutamine, (10) glutamic acid, (11) proline, (12) valine, (13) methionine, (14) isoleucine, (15) leucine, (16) tyrosine, (17) phenylalanine, (18) tryptophan, (19)  $\text{N}_2$ -glutamine, and (20) aspartic acid.

population, whereas the corrected  $m + 1$  peak area, or in the case of Gln and Asn, the sum of corrected peak areas for  $m + 1$  and  $m + 2$ , represent the  $^{15}\text{N}$  amino acid population. The  $^{15}\text{N}$  amino acid enrichment was calculated according to the equation reported by Gaudin et al.<sup>23</sup> Briefly, the  $^{15}\text{N}$  isotopologue enrichment of each amino acid was calculated by taking into account the endogenous amino acid as well as newly synthesized amino acid. The equation for estimating the isotopologue enrichment is given as

$$\frac{\frac{[^{15}\text{N AA}_{\text{sample}}]}{[[^{14+15}\text{N AA}_{\text{sample}}]]}}{\frac{[^{15}\text{N AA}_{\text{control}}]}{[[^{14+15}\text{N AA}_{\text{control}}]]}} = \frac{\frac{a_1 \times ^{15}\text{N AA}_{\text{sample area MRM}}}{a_1 \times ^{15}\text{N AA}_{\text{sample area MRM}} + a_2 \times ^{14}\text{N AA}_{\text{sample area MRM}}}}{\frac{a_1 \times ^{15}\text{N AA}_{\text{control area MRM}}}{a_1 \times ^{15}\text{N AA}_{\text{control area MRM}} + a_2 \times ^{14}\text{N AA}_{\text{control area MRM}}}}$$

where  $a_1$  is the slope corresponding to labeled ( $^{15}\text{N}$ ) amino acid standards calibration curve and  $a_2$  is the slope corresponding to unlabeled ( $^{14}\text{N}$ ) amino acid standards calibration curve; control represents plants supplied with  $^{14}\text{N}$  ammonium nitrate, and sample represents plants supplied with  $^{15}\text{NH}_4^{15}\text{NO}_3$ ; area MRM represents the area under the curve for the amino acid multiple reaction monitoring (MRM).

**Statistical Analyses.** Univariate statistical analysis (Student's  $t$  test, ANOVA) was performed to determine the statistical significance of amino acid pools among the different treatment groups (biotypes and herbicide) followed by Tukey's HSD post hoc test. Statistical significance of the BCA assay was tested by two-way analysis of variance. Differences among individual means were tested using Tukey's HSD multiple-comparison tests with  $P$  value  $< 0.05$  considered statistically significant. Statistical analyses were performed using SAS v 9.2 (SAS Institute, Cary, NC, USA). For the metabolic profiling analysis, metabolomics data were auto-scaled to satisfy the assumptions of normality and equal variance before multivariate analyses. Supervised partial least squares-discriminant analysis (PLS-DA) models were constructed using MetaboAnalyst to test the significance of the effects of biotype and herbicide treatments on the metabolite profiles.<sup>24</sup> Hierarchical cluster analysis, using Pearson distance as the similarity measure, of the metabolite responses with respect to the treatments was visualized using a heatmap generated from MetaboAnalyst software.

## RESULTS AND DISCUSSION

In this study, we report the effect of the EPSPS-targeting herbicide, glyphosate, on plant nitrogen metabolism using stable isotope-resolved metabolomic (SIRM) analysis. The metabolism of two biotypes of *A. palmeri* that are susceptible (S-) and resistant (R-) to glyphosate was evaluated by quantitative analysis of  $^{15}\text{N}$  amino acid-enriched isotopologues after  $^{15}\text{N}$ -ammonium nitrate had been supplied to plants immediately after exposure to glyphosate. Even though the RounUp ProMax that was used in this study contain 51% of non active ingredient, the nitrate, ammonium and amino acid concentration of the spray solution were below 0.01 ppm. Hence the ammonium nitrate applied to the modified MS solution was the only source of N available to the plants after treatment application. Of the 20 physiological amino acids, 19  $^{14}\text{N}$  amino acids, with the exception of cysteine, and 18  $^{15}\text{N}$  amino acids, with the exceptions of cysteine and glycine, were identified and resolved using mass spectrometry (Figure 1). Consistent with previously reported observations in *A. palmeri* populations,<sup>20,25</sup> a significant accumulation of amino acids was

observed in the S-biotype following glyphosate application. The total amino acid pool doubled in the S-biotype 36 h after glyphosate application, whereas the observed increase in the total amino acid pool of R-biotype was statistically non-significant (Figure 2). Similar observations of amino acid accumulation in glyphosate-sensitive plants following exposure to glyphosate have been previously reported.<sup>12,26</sup>

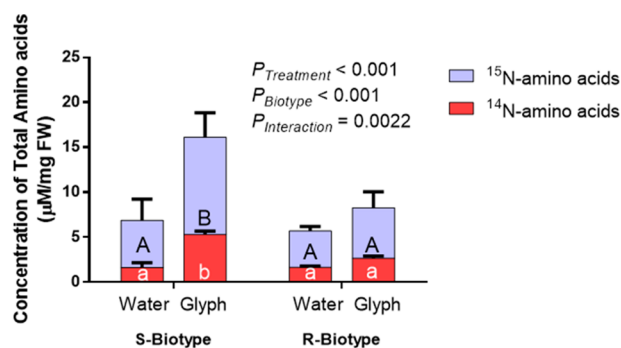


**Figure 2.** Relative proportions of  $^{14}\text{N}$  and  $^{15}\text{N}$  amino acids in S- and R-biotypes of *A. palmeri* grown in  $^{15}\text{N}$ -supplemented MS solution. The data represent the relative proportions of  $^{14}\text{N}$  and  $^{15}\text{N}$  amino acids in water and glyphosate-treated S- and R-biotypes of *A. palmeri* harvested at 36 HAT. The bars represent the mean  $\pm 1$  SD of total free amino acids, and the mean  $\pm 1$  SD was tested by Tukey's HSD. Means with different letters are significantly different at  $p < 0.05$  (two-way ANOVA followed by Tukey's HSD test,  $P < 0.05$ ). Letters A and B represent significant differences between  $^{15}\text{N}$  amino acids, whereas letters a and b represent significant differences between  $^{14}\text{N}$  amino acids.

Because the S-biotype is highly susceptible to glyphosate ( $\text{GR}_{50} = 0.09$  kg ae/ha), the observed increase of the amino acid pool following glyphosate application is thought to be primarily caused by accelerated protein catabolism and decreased downstream utilization of amino acids for protein synthesis. The argument favoring lower protein synthesis and/or higher protein catabolism in glyphosate-treated S-biotype is supported by the observation of lower concentration of total soluble protein (TSP) (Figure 3). While the total content of TSP decreased by 43% in the glyphosate-treated S-biotype compared to its water-treated control (Figure 3). However, there was no statistically significant difference in the TSP content between the water-treated control and glyphosate-treated R-biotype. Increased protein catabolism is further supported by the concomitant doubling of the  $^{14}\text{N}$  amino acid pools in the glyphosate-treated S-biotype compared to that of the water-treated S-biotype (Figure 2). However, the proportional abundance of  $^{15}\text{N}$ -labeled amino acids also doubled in glyphosate-treated S-biotype compared to that of water-treated control. This increased  $^{15}\text{N}$  amino acid pool indicates an increase in the de novo amino acid synthesis, coupled with a lower protein synthesis rate in the S-biotype following glyphosate exposure. Thus, the SIRM data suggest that the increase in amino acid pool in the S-biotype following

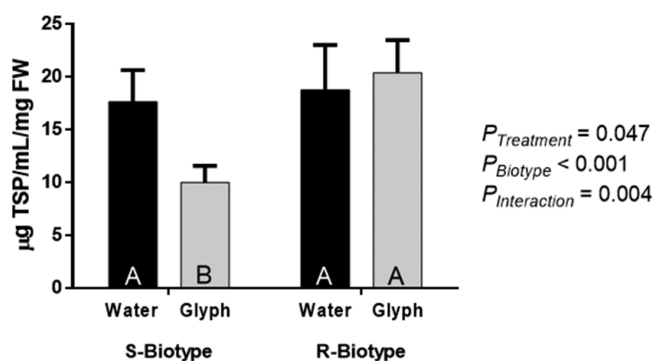


**Figure 3.** Total soluble protein (TSP) concentration estimation by BCA assay: concentration of TSPs in water and herbicide-treated S- and R-biotypes of *A. palmeri* grown in  $^{15}\text{N}$ -supplemented MS solution. The data represent the mean  $\pm$  1 SD of concentration of TSPs, and the mean  $\pm$  1 SD was tested by Tukey's HSD. Means with different letters are significantly different at  $p < 0.05$  (two-way ANOVA followed by Tukey's HSD test,  $P < 0.05$ ).

glyphosate application is contributed not only by protein catabolism but also through an increase in the de novo amino acid synthesis coupled with a potentially lower protein synthesis. Compared to the herbicide-treated S-biotype, the relatively lower abundance of  $^{15}\text{N}$  amino acid in the herbicide-treated R-biotype could be potentially attributed to a lower perturbation in protein synthesis, which is supported by its similar relative abundances of  $^{14}\text{N}$  and  $^{15}\text{N}$  amino acids (Figure 2) and TSP (Figure 3) in both herbicide-treated and water-treated R-biotype.

Examination of the  $^{15}\text{N}$  amino acid enrichment profile of the glyphosate-treated S-biotype showed a significant decrease in the abundance of the aromatic amino acids, which is consistent with the inhibition of the shikimate pathway as shown in Figure S1 of the Supporting Information. The glyphosate-treated S-biotype also revealed that the elevated isotopologue abundance of the total  $^{15}\text{N}$  amino acid pool was primarily contributed to by the abundance of  $^{15}\text{N}$ -asparagine (Asn),  $^{15}\text{N}$ -glutamine (Gln),  $^{15}\text{N}$ -alanine (Ala), and  $^{15}\text{N}$ -serine (Ser) (Figure 4).

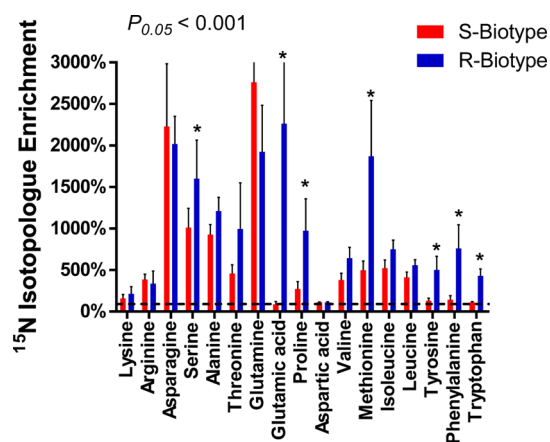


**Figure 4.**  $^{15}\text{N}$  isotopologue enrichment of amino acids in glyphosate-treated S- and R-biotypes of *A. palmeri* harvested at 36 HAT. The data represent the mean  $\pm$  1 SD of each amino acid. Statistical significance of the mean was determined by paired  $t$  test at a confidence level of 0.05. The dotted line (100%) corresponds to natural  $^{15}\text{N}$  isotopologue enrichment of amino acids. The \* indicates significant difference at  $p < 0.05$  in the  $^{15}\text{N}$  isotopologue enrichment (Student's  $t$  test).

These four amino acids, synthesized through shikimate-independent pathways, together constituted about 53% of the total amino acid abundance in the glyphosate-treated S-biotype. These observations are in agreement with reports of similar abundance of these four amino acids in plants exposed to various abiotic stresses.<sup>27–29</sup> However, our results, which document a relative abundance of  $^{15}\text{N}$  isotopologue of these amino acids, indicate that the increase in their concentration (Figure 4) could partly be attributed to de novo synthesis rather than protein catabolism alone. The significantly lower isotopologue enrichment of aromatic amino acids in glyphosate-treated S- compared to R-biotype was expected. However, this study also indicated that synthesis of serine, proline (a stress-related amino acid), glutamic acid, and methionine in the glyphosate treated S-biotype was significantly reduced as an indirect result of inhibition of EPSPS enzyme.

Physiologically, biosynthetic pathways of all nitrogenous compounds are linked with either glutamine or its acidic counterpart, glutamate.<sup>30</sup> Glutamine, a primary amino group donor for most N compounds, is derived from the processes of primary nitrogen assimilation (Figure 5) involving glutamate and ammonia, and is regulated by several enzymes including the glutamine synthetase/glutamate synthase (GS/GOGAT) enzyme complex.<sup>31,32</sup> The increase in  $^{15}\text{N}$ -enriched Gln in response to herbicide application in both S- and R-biotypes indicates an increase in its biosynthesis, potentially driven by downstream sink strength. However, despite the assimilation of inorganic nitrogen into Gln in the glyphosate-treated S-biotype, disruption of the carbon metabolism, as evidenced by higher sugar accumulation (Figure 6), could interrupt the transport of amino acids to various organellar sites.<sup>32,33</sup> The GS/GOGAT pathway is of crucial importance in plants, because the Gln and Glu are donors for the biosynthesis of major N-containing compounds, including amino acids, nucleotides, and polyamines.<sup>34</sup> The glutamine/glutamate (Gln/Glu) ratio is a good indicator of the balance between the capacity for C and N assimilation and N availability for biosynthesis of organic nitrogen compounds.<sup>35,36</sup> A lower Gln/Glu ratio indicates a higher de novo amino acid synthesis.<sup>37–39</sup> The herbicide-treated R-biotype had a Gln/Glu ratio of about 1.4, and was similar to that in the control S- and R-biotypes, whereas the herbicide-treated S-biotype had a 10-fold increase in the Gln/Glu ratio (Figure 7A). The higher ratio indicates an accumulation of glutamine synthesized during the early process of nitrogen assimilation, coupled with a decreased synthesis of glutamate.<sup>26</sup> As the synthesis of glutamate is primarily dependent on the level of 2-oxoglutarate (2-OG,  $\alpha$ -ketoglutarate), decreased availability of 2-OG would hamper the synthesis of Glu. The decreased synthesis of glutamate in the glyphosate-treated S-biotype, compared to the R-biotype, can thus be attributed to the lower availability of  $\alpha$ -ketoglutarate (Figure 7B). Furthermore, inorganic nitrogen in plants is assimilated initially to Asn and Gln, and these amino acids serve as important nitrogen carriers.<sup>12,40</sup> The relatively higher abundance of these amino acids in the glyphosate-treated S- and R-biotypes, compared to other amino acids, could indicate that the initial assimilation of  $\text{NH}_3$  to amino acids is enhanced by glyphosate treatment, even though protein synthesis is hampered by the herbicide in the S-biotype (Figure 3). Significant accumulation of Asn has been reported in plants subjected to various abiotic stresses, even though they are these plants are unable to maintain protein synthesis.<sup>41,42</sup>

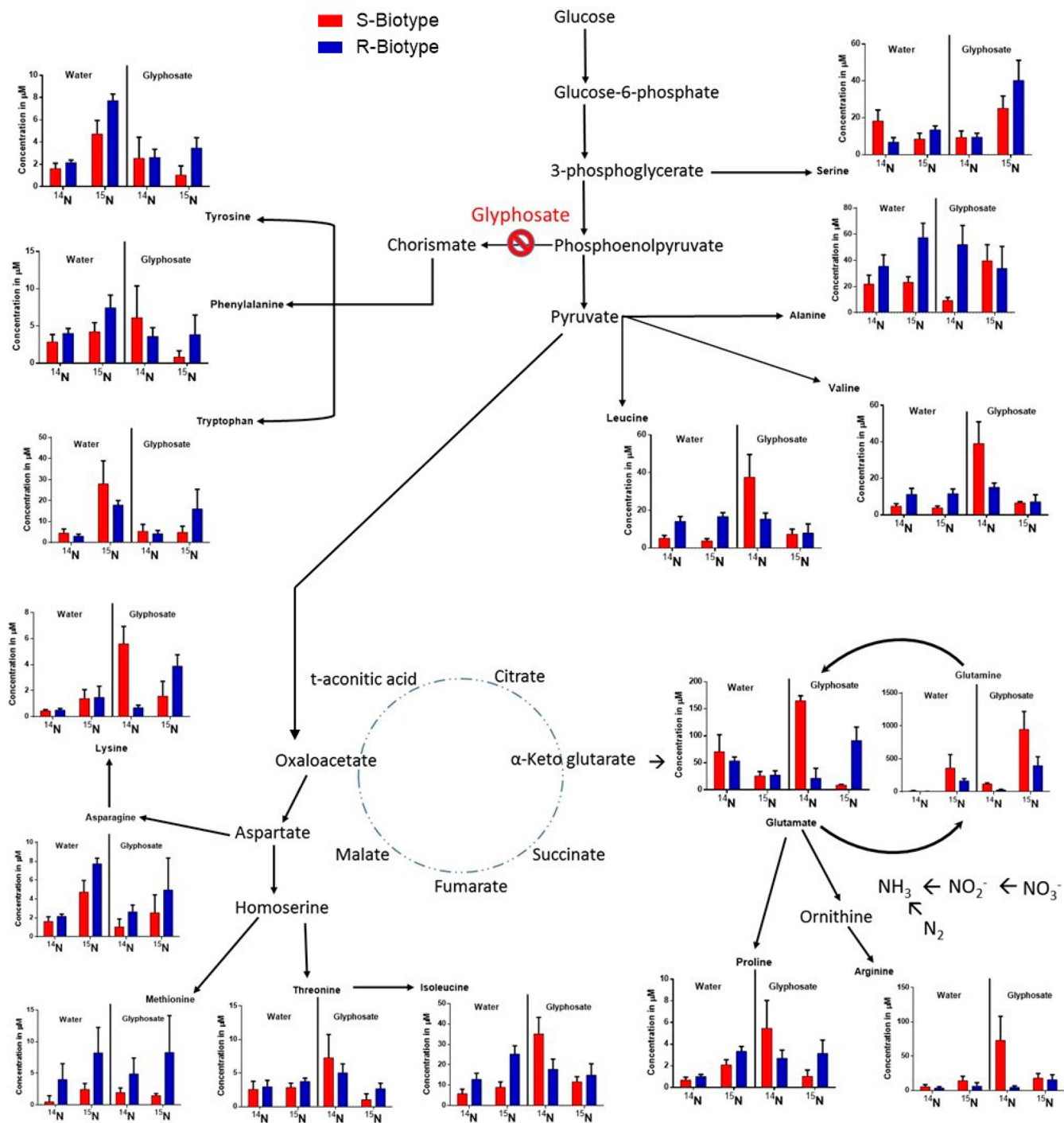


**Figure 5.** Amino acid biosynthesis pathway: concentration of  $^{15}\text{N}$ - and  $^{14}\text{N}$ -incorporated amino acid profile biosynthesis pathways in water- and herbicide-treated S- and R-biotypes of *A. palmeri* grown in  $^{15}\text{N}$ -supplemented solution and harvested at 36 HAT. The left half of each graph represents the  $^{14}\text{N}$  and  $^{15}\text{N}$  amino acid levels in water treatment, and the right half represents the  $^{14}\text{N}$  and  $^{15}\text{N}$  amino acid levels in glyphosate treatment. The data represent the mean  $\pm$  1 SD of each amino acid.

As most amino acids are primarily derived from precursors of carbon metabolism (pyruvate, phosphoenolpyruvate, oxaloacetate, and  $\alpha$ -ketoglutarate), perturbations in the carbon–nitrogen homeostasis (Figure 6) would lead to disruptions in the global transregulation of amino acid metabolism in the susceptible biotypes (Figures 4 and 5). In response to herbicide application, a general increase in total free amino acid content with a transient decrease in the proportion of the amino acids whose pathways are specifically inhibited is commonly

observed.<sup>12</sup> The primary outcome of EPSPS inhibition is aromatic amino acid pool depletion. Consistent with this, the abundance of aromatic amino acids in the S-biotype decreased by 82% in comparison to the R-biotype, which had only a 25% decrease, as shown in Figure S1 of the Supporting Information. This decrease of aromatic amino acids in the R-biotype can be attributed to the initial transient inhibitory effect of glyphosate on the shikimate pathway.<sup>20</sup> Furthermore, the EPSPS-targeting herbicide is structurally analogous to phosphoenolpyruvate

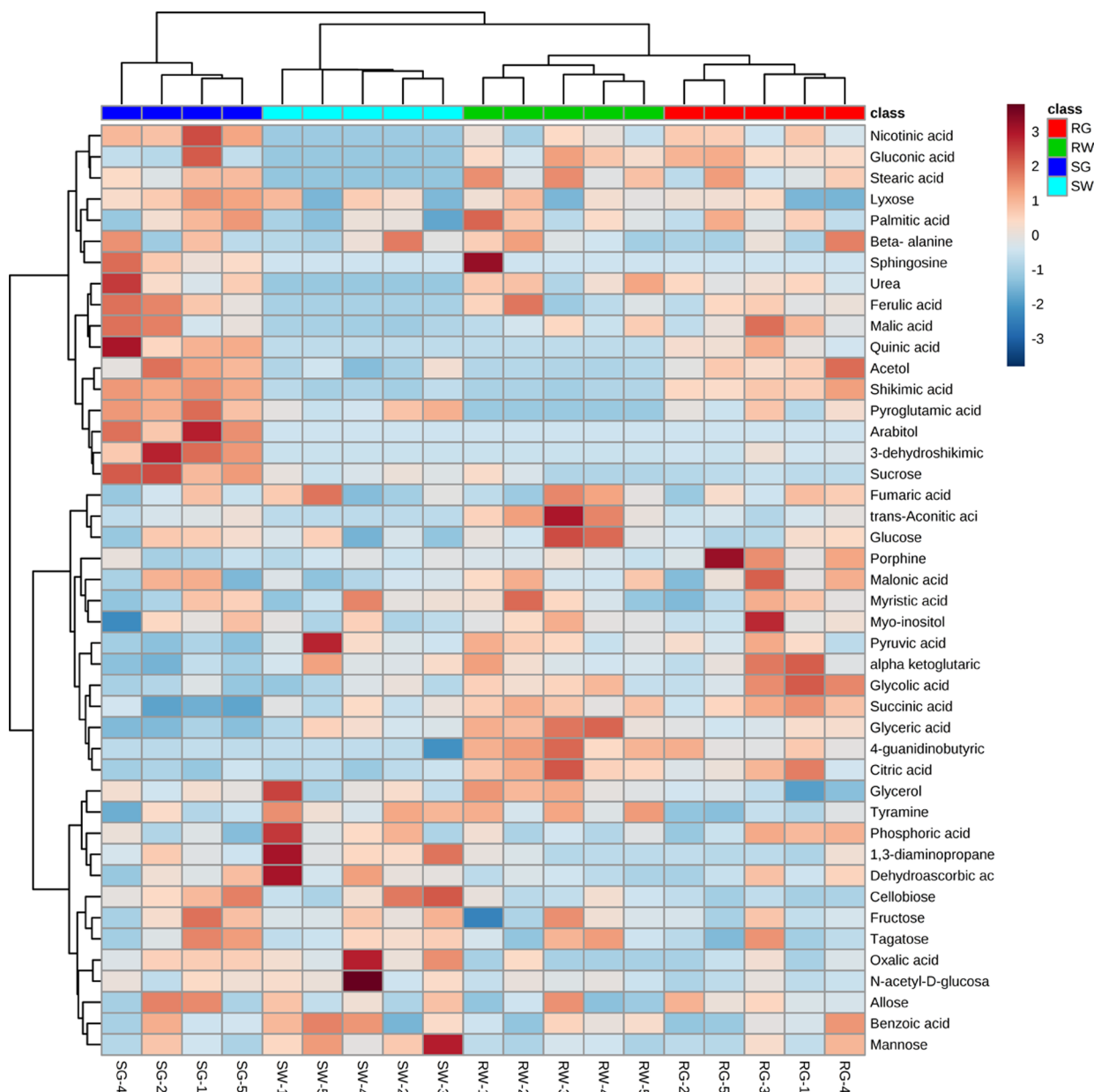


**Figure 6.** Hierarchical cluster analysis of metabolites in S- and R-biotypes of *A. palmeri*: heatmap depiction of two-way hierarchical clustering of total sugars, shikimate pathway, and tricarboxylic acid (TCA) cycle metabolites in leaves of water- and herbicide-treated S- and R-biotypes of *A. palmeri* grown in  $^{15}\text{N}$ -supplemented MS solution and harvested at 36 HAT. The algorithm for heatmap clustering was based on Euclidean distance measure for similarity and Ward linkage method for biotype clustering. SG, RG, glyphosate-treated S- and R-biotype, respectively; SW, RW, water-treated S- and R-biotype, respectively.

(PEP) and competes with PEP for the EPSPS enzyme, and hence could result in the potential accumulation of PEP. Thus, the enhanced abundance of  $^{15}\text{N}$ -Ala and  $^{15}\text{N}$ -Ser in the glyphosate-treated S-biotype could be potentially attributed to the transamination of glycolytic intermediates of pyruvate and 3-phosphoglycerate, respectively, via the carboxylation of the under-utilized PEP.<sup>43</sup>

The observations from this study suggest that the chemical stress-induced increase in the amino acid pool in the S-biotype is partly caused by the de novo synthesis of amino acids involved in early transamination reactions. Furthermore, the effect of inhibiting EPSPS is not restricted to inhibition of aromatic amino acid biosynthesis alone, it also disrupts the de novo biosynthesis of most nonaromatic acids as a consequence

of deregulation of the shikimate pathway. Thus, the elevated amino acid pool observed in the S-biotype could be an amalgamation of both anabolic and catabolic processes. In contrast, in the R-biotype, the amino acid pool is enriched primarily by anabolic processes, and this elevated synthesis of amino acids in the R-biotype potentially complements the resistance mechanisms occurring in this biotype conferred via increased *EPSPS* gene copy number and elevated enzymatic and nonenzymatic antioxidant mechanisms.<sup>19,20</sup> Our results indicate that the stress-induced amino acid accumulation in plants is not solely due to proteolysis but also contributed by de novo synthesis following nitrogen assimilation. However, diminished physiological activities result in decreased protein synthesis and, hence, the newly synthesized amino acids

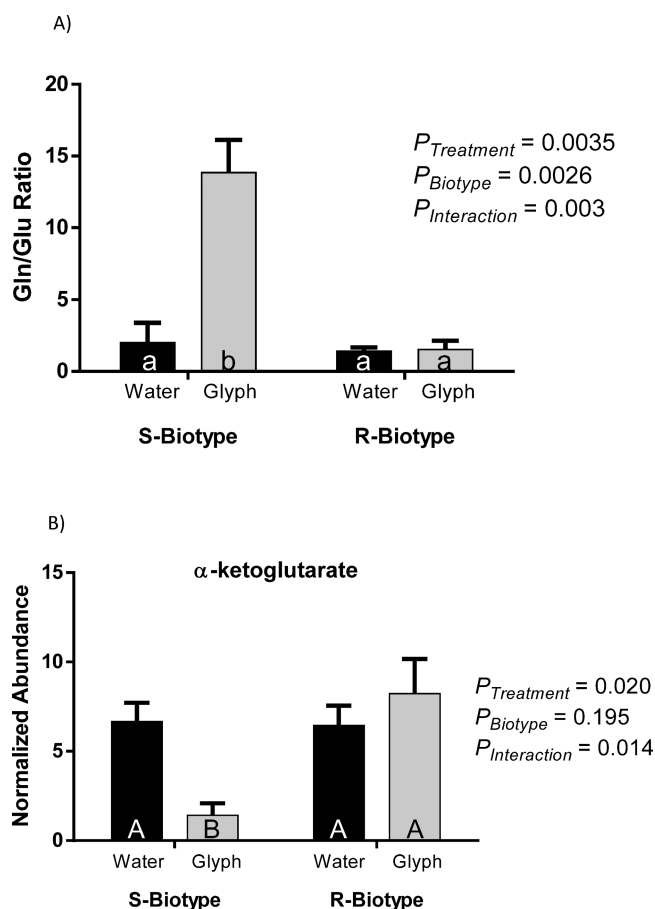


**Figure 7.** Regulation of GS-GOGAT cycle metabolites in response to glyphosate application in S- and R-biotypes of *A. palmeri* grown in  $^{15}\text{N}$ -supplemented MS solution. (A) Gln/Glu ratio in water- and herbicide-treated S- and R-biotypes of *A. palmeri* harvested at 36 HAT. (B) Relative abundance of  $\alpha$ -ketoglutarate (2-oxoglutarate) in water- and herbicide-treated S- and R-biotypes of *A. palmeri* harvested at 36 HAT. The data represent the mean  $\pm$  1 SD of each amino acid. The mean  $\pm$  1 SD was tested by Tukey's HSD comparing across all treatments at a confidence level of 0.05. Means with different letters are significantly different at  $P < 0.05$  (two-way ANOVA, Tukey's HSD).

accumulate. Furthermore, our results indicate that although glyphosate is a-specific inhibitor of a shikimate pathway enzyme, interactions between the various amino acid synthesis pathways may ensure resource allocation for de novo synthesis of amino acids as a means of stress mitigation. Conversely, the disruption of nitrogen metabolism outside the shikimate pathway after inhibition of EPSPS may partly initiate the processes that ultimately lead to cell death in glyphosate-treated susceptible plants.

## ■ ASSOCIATED CONTENT

### 📄 Supporting Information

The Supporting Information is available free of charge on the ACS Publications website at DOI: 10.1021/acs.jafc.6b02196.

Table of fragment ions and isotopic mass abundance (%) used for correction of amino acid abundance for  $^{15}\text{N}$ -amino acid isotopologue enrichment analysis and a graph depicting the concentration of  $^{15}\text{N}$ - and  $^{14}\text{N}$ -aromatic amino acids in S- and R-biotypes of *Amaranthus palmeri* (PDF)

## ■ AUTHOR INFORMATION

### Corresponding Author

\*(N.T.) Phone: (864) 656-4453. E-mail: [ntharay@clermson.edu](mailto:ntharay@clermson.edu).

### Notes

The authors declare no competing financial interest.

## ■ ACKNOWLEDGMENTS

We thank Patrick Gerard for assisting with statistical analysis of the experimental data. This is technical Contribution No. 6455 of the Clemson University Experiment Station, under project number SC-17000505.

## ■ ABBREVIATIONS USED

EPSPS, 5-enolpyruvylshikimate-3-phosphate synthase; HAT, hours after treatment;  $\text{GR}_{50}$ , glyphosate rate causing 50% reduction in biomass; TSP, total soluble proteins; MRM, multiple reaction monitoring; TCA, tricarboxylic acid cycle; PEP, phosphoenolpyruvate; 2-OG, 2-oxoglutarate; GS/GOGAT, glutamine synthetase/glutamate synthase

## ■ REFERENCES

- (1) Less, H.; Galili, G. Principal transcriptional programs regulating plant amino acid metabolism in response to abiotic stresses. *Plant Physiol.* **2008**, *147*, 316–330.
- (2) Araújo, W. L.; Tohge, T.; Ishizaki, K.; Leaver, C. J.; Fernie, A. R. Protein degradation – an alternative respiratory substrate for stressed plants. *Trends Plant Sci.* **2011**, *16*, 489–498.
- (3) Zulet, A.; Gil-Monreal, M.; Villamor, J. G.; Zabalza, A.; van, d.H.; Royuela, M. Proteolytic pathways induced by herbicides that inhibit amino acid biosynthesis. *PLoS One* **2013**, *8*, e73847.
- (4) Hildebrandt, T. M.; Nesi, A. N.; Araújo, W. L.; Braun, H. Amino acid catabolism in plants. *Mol. Plant* **2015**, *8*, 1563–1579.
- (5) Delauney, A. J.; Verma, D. P. S. Proline biosynthesis and osmoregulation in plants. *Plant J.* **1993**, *4*, 215–223.
- (6) Rai, V. K. Role of amino acids in plant responses to stresses. *Biol. Plant.* **2002**, *45*, 481–487.
- (7) Bari, R.; Jones, J. D. G. Role of plant hormones in plant defence responses. *Plant Mol. Biol.* **2009**, *69*, 473–488.
- (8) Duke, S. O. Perspectives on transgenic, herbicide-resistant crops in the United States almost 20 years after introduction. *Pest Manage. Sci.* **2015**, *71*, 652–657.
- (9) Duke, S. O.; Powles, S. B. Glyphosate: a once-in-a-century herbicide. *Pest Manage. Sci.* **2008**, *64*, 319–325.
- (10) Gomes, M. P.; Smedbol, E.; Chalifour, A.; Henault-Ethier, L.; Labrecque, M.; Lepage, L.; Lucotte, M.; Juneau, P. Alteration of plant physiology by glyphosate and its by-product aminomethylphosphonic acid: an overview. *J. Exp. Bot.* **2014**, *65*, 4691–4703.
- (11) Yannicari, M.; Istilart, C.; Giménez, D. O.; Castro, A. M. Effects of glyphosate on the movement of assimilates of two *Lolium perenne* L. populations with differential herbicide sensitivity. *Environ. Exp. Bot.* **2012**, *82*, 14–19.
- (12) Orcaray, L.; Igal, M.; Marino, D.; Zabalza, A.; Royuela, M. The possible role of quinate in the mode of action of glyphosate and acetolactate synthase inhibitors. *Pest Manage. Sci.* **2010**, *66*, 262–269.
- (13) Armendáriz, O.; Gil-Monreal, M.; Zulet, A.; Zabalza, A.; Royuela, M. Both foliar and residual applications of herbicides that inhibit amino acid biosynthesis induce alternative respiration and aerobic fermentation in pea roots. *Plant Biol. (Berlin, Ger.)* **2016**, *18*, 382–390.
- (14) Moldes, C. A.; Medici, L. O.; Abrahão, O. S.; Tsai, S. M.; Azevedo, R. A. Biochemical responses of glyphosate resistant and susceptible soybean plants exposed to glyphosate. *Acta Physiol. Plant.* **2008**, *30*, 469–479.



- (15) Jaworski, E. G. Mode of action of *N*-phosphonomethylglycine. Inhibition of aromatic amino acid biosynthesis. *J. Agric. Food Chem.* **1972**, *20*, 1195–1198.
- (16) Forlani, G.; Kafarski, P.; Lejczak, B.; Wieczorek, P. Mode of action of herbicidal derivatives of aminomethylenebisphosphonic acid. Part II. Reversal of herbicidal action by aromatic amino acids. *J. Plant Growth Regul.* **1997**, *16*, 147–152.
- (17) Petersen, I. L.; Hansen, H. C. B.; Ravn, H. W.; Sørensen, J. C.; Sørensen, H. Metabolic effects in rapeseed (*Brassica napus* L.) seedlings after root exposure to glyphosate. *Pestic. Biochem. Physiol.* **2007**, *89*, 220–229.
- (18) Moldes, C. A.; Camiña, J. M.; Medici, L. O.; Tsai, S. M.; Azevedo, R. A. Physiological effects of glyphosate over amino acid profile in conventional and transgenic soybean (*Glycine max*). *Pestic. Biochem. Physiol.* **2012**, *102*, 134–141.
- (19) Nandula, V. K.; Reddy, K. N.; Koger, C. H.; Poston, D. H.; Rimando, A. M.; Duke, S. O.; Bond, J. A.; Ribeiro, D. N. Multiple resistance to glyphosate and pyriithiobac in Palmer amaranth (*Amaranthus palmeri*) from Mississippi and response to flumiclorac. *Weed Sci.* **2012**, *60*, 179–188.
- (20) Maroli, A. S.; Nandula, V. K.; Dayan, F. E.; Duke, S. O.; Gerard, P.; Tharayil, N. Metabolic profiling and enzyme analyses indicate a potential role of antioxidant systems in complementing glyphosate resistance in an *Amaranthus palmeri* biotype. *J. Agric. Food Chem.* **2015**, *63*, 9199–9209.
- (21) MS-Isotope, <http://prospector.ucsf.edu/prospector/cgi-bin/msform.cgi?form=msisotopehttp://prospector.ucsf.edu/ucsfhtml3.4/msiso.htm> (accessed July 17, 2016).
- (22) Alexova, R.; Nelson, C. J.; Jacoby, R. P.; Millar, A. H. Exposure of barley plants to low Pi leads to rapid changes in root respiration that correlate with specific alterations in amino acid substrates. *New Phytol.* **2015**, *206*, 696–708.
- (23) Gaudin, Z.; Cerveau, D.; Marnet, N.; Bouchereau, A.; Delavault, P.; Simier, P.; Pouvreau, J. B. Robust method for investigating nitrogen metabolism of <sup>15</sup>N labeled amino acids using Accq• Tag ultra performance liquid chromatography-photodiode array-electrospray ionization-mass spectrometry: application to a parasitic plant-plant interaction. *Anal. Chem.* **2014**, *86*, 1138–1145.
- (24) Xia, J.; Sinelnikov, I. V.; Han, B.; Wishart, D. S. MetaboAnalyst 3.0 – making metabolomics more meaningful. *Nucleic Acids Res.* **2015**, *43*, 251–257.
- (25) Fernandez-Escalada, M.; Gil-Monreal, M.; Zabalza, A.; Royuela, M. Characterization of the *Amaranthus palmeri* physiological response to glyphosate in susceptible and resistant populations. *J. Agric. Food Chem.* **2016**, *64*, 95–106.
- (26) Vivancos, P. D.; Driscoll, S. P.; Bulman, C. A.; Ying, L.; Emami, K.; Treumann, A.; Mauve, C.; Noctor, G.; Foyer, C. H. Perturbations of amino acid metabolism associated with glyphosate-dependent inhibition of shikimic acid metabolism affect cellular redox homeostasis and alter the abundance of proteins involved in photosynthesis and photorespiration. *Plant Physiol.* **2011**, *157*, 256–268.
- (27) Rhodes, D.; Hogan, A. L.; Deal, L.; Jamieson, G. C.; Haworth, P. Amino acid metabolism of *Lemna minor* L. II. Responses to chlorsulfuron. *Plant Physiol.* **1987**, *84*, 775–780.
- (28) Fougère, F.; Le Rudulier, D.; Streeter, J. G. Effects of salt stress on amino acid, organic acid, and carbohydrate composition of roots, bacteroids, and cytosol of alfalfa (*Medicago sativa* L.). *Plant Physiol.* **1991**, *96*, 1228–1236.
- (29) Martinelli, T.; Whittaker, A.; Bochicchio, A.; Vazzana, C.; Suzuki, A.; Masclaux-Daubresse, C. Amino acid pattern and glutamate metabolism during dehydration stress in the ‘resurrection’ plant *Sporobolus stapfianus*: a comparison between desiccation-sensitive and desiccation-tolerant leaves. *J. Exp. Bot.* **2007**, *58*, 3037–3046.
- (30) Bernard, S. M.; Habash, D. Z. The importance of cytosolic glutamine synthetase in nitrogen assimilation and recycling. *New Phytol.* **2009**, *182*, 608–620.
- (31) Reyes-Prieto, A.; Moustafa, A. Plastid-localized amino acid biosynthetic pathways of Plantae are predominantly composed of non-cyanobacterial enzymes. *Sci. Rep.* **2012**, *2*, 955.
- (32) Pratelli, R.; Pilot, G. Regulation of amino acid metabolic enzymes and transporters in plants. *J. Exp. Bot.* **2014**, *65*, 5535–5556.
- (33) Orcaray, L.; Zulet, A.; Zabalza, A.; Royuela, M. Impairment of carbon metabolism induced by the herbicide glyphosate. *J. Plant Physiol.* **2012**, *169*, 27–33.
- (34) Lea, P. J.; Ireland, R. J. Nitrogen metabolism in higher plants. In *Plant Amino Acids: Biochemistry and Biotechnology*, 1; Singh, B. K., Ed.; Dekker: New York, 1999; pp 1–47.
- (35) Lancien, M.; Gadal, P.; Hodges, M. Enzyme redundancy and the importance of 2-oxoglutarate in higher plant ammonium assimilation. *Plant Physiol.* **2000**, *123*, 817–824.
- (36) Flynn, K. J. Nutrient limitation of marine microbial production: fact or artefact? *Chem. Ecol.* **1989**, *4*, 1–13.
- (37) Flynn, K. J.; Dickson, D. M. J.; Al-Amoudi, O. The ratio of glutamine: glutamate in microalgae: a biomarker for N-status suitable for use at natural cell densities. *J. Plankton Res.* **1989**, *11*, 165–170.
- (38) Novitskaya, L.; Trevanion, S. J.; Driscoll, S.; Foyer, C. H.; Noctor, G. How does photorespiration modulate leaf amino acid contents? A dual approach through modelling and metabolite analysis. *Plant, Cell Environ.* **2002**, *25*, 821–835.
- (39) Foyer, C. H.; Parry, M.; Noctor, G. Markers and signals associated with nitrogen assimilation in higher plants. *J. Exp. Bot.* **2003**, *54*, 585–593.
- (40) Lam, H. M.; Hsieh, M. H.; Coruzzi, G. Reciprocal regulation of distinct asparagine synthetase genes by light and metabolites in *Arabidopsis thaliana*. *Plant J.* **1998**, *16*, 345–353.
- (41) Jia, M.; Keutgen, N.; Matsushashi, S.; Mitzuniwa, C.; Ito, T.; Fujimura, T.; Hashimoto, S. Ion chromatographic analysis of selected free amino acids and cations to investigate the change of nitrogen metabolism by herbicide stress in soybean (*Glycine max*). *J. Agric. Food Chem.* **2001**, *49*, 276–280.
- (42) Lea, P. J.; Sodek, L.; Parry, M. A.; Shewry, P. R.; Halford, N. G. Asparagine in plants. *Ann. Appl. Biol.* **2007**, *150*, 1–26.
- (43) O’Leary, B.; Paxton, W. C. The central role of glutamate and aspartate in the post-translational control of respiration and nitrogen assimilation in plant cells. In *Amino Acids in Higher Plants*; D’Mello, J. F., Ed.; CABI: Boston, MA, USA, 2015; pp 277–297.